Dalton Transactions

RSC Publishing

PAPER

View Article Online
View Journal | View Issue

Cite this: *Dalton Trans.*, 2013, **42**, 6142

Copper(II) chemistry of the functionalized macrocycle cyclam tetrapropionic acid†

Peter Comba,*[a] Franziska Emmerling,[b] Maik Jakob,[a] Werner Kraus,[b] Manja Kubeil,[c] Michael Morgen,[a] Jens Pietzsch[c,d] and Holger Stephan*[c]

Received 5th October 2012,
Accepted 26th November 2012

DOI: 10.1039/c2dt32356g

www.rsc.org/dalton

The Cu^{II} complex of H_4TETP (H_4TETP = 1,4,8,11-tetraazatetradecane-1,4,8,11-tetrapropionic acid) is five-coordinate with a distorted square-pyramidal structure (τ = 0.45; *i.e.* the geometry is nearly half-way between square-pyramidal and trigonal-bipyramidal) and a relatively long Cu–N and a short Cu–O bond; the comparison between powder and solution electronic spectroscopy, the frozen solution EPR spectrum and ligand-field-based calculations (angular overlap model, AOM) indicate that the solution and solid state structures are very similar, *i.e.* the complex has a relatively low "in-plane" and a significant axial ligand field with a $d_{x^2-y^2}$ ground state. The ligand-enforced structure is therefore shown to lead to a partially quenched Jahn–Teller distortion and to a relatively low complex stability, lower than with the corresponding acetate-derived ligand H_4TETA. This is confirmed by potentiometric titration and by the biodistribution with ^{64}Cu-labeled ligands which show that the uptake in the liver is significantly increased with the H_4TETP-based system.

Introduction

In recent years, positron emission tomography (PET) developed to an important diagnostic tool for the visualization of biological processes within living systems and in particular in oncology.[1–3] Among the non-traditional metal-based positron emitting radionuclides, copper-64 is one of the most intensively evaluated isotopes, and this is due to its decay properties and lifetime (β^+, 19%; β^-, 40%; electron capture, 40%, $t_{1/2}$ = 12.7 h) as well as its increasing availability and production, the advantages of the ^{64}Cu/^{67}Cu matched pair (diagnosis and therapy) and the large knowledge base in copper coordination chemistry.[4–8] An important focus is on the development of radio-labeled biomolecules such as antibodies, proteins and peptides as targeting vectors, and this requires bifunctional chelators (BFC's), *i.e.* ligands which tightly bind the radiometal ion and have a covalent conjugation to the biomolecule.

Tetraazamacrocyclic ligands, especially cyclam derivatives (cyclam = 1,4,8,11-tetraazatetradecane), specifically but not exclusively with acetate-substituted tertiary amine donor groups are among the most widely used BFC's,[8] and this is due to the high stability of $[Cu(cyclam)]^{2+}$.[9] Apart from substituted cyclam derivatives, cross- and side-bridged tetraazamacrocycles have been shown to lead to higher stabilities, kinetic inertness and better resistance to $Cu^{II/I}$ reduction,[10–15] and other ligands such as the sar-type hexaaza cages,[16–19] triazacyclononane derivatives,[20] and bispidine-type ligands[21,22] have also been studied extensively, with various advantages in terms of the formation kinetics, thermodynamic stabilities, ease of biovector substitution and *in vivo* properties.

Here, we report the synthesis and copper(II) coordination chemistry of H_4TETP (H_4TETP = cyclam-1,4,8,11-tetrapropionic acid).[23–25] Solution spectroscopy and a single crystal X-ray structural analysis indicate that one of the four propionate pendant groups is coordinated axially to the metal center, while the other three are dangling and available for further derivatization, resulting in a distorted square-pyramidal coordination geometry. In comparison to the well-studied acetate derivatives of cyclam,[10–14] this is an unusual coordination mode, and possible reasons and implications with respect to applications for radiolabeling of biovectors and PET are analyzed and discussed.

[a]*Universität Heidelberg, Anorganisch-Chemisches Institut, INF 270, D-69120 Heidelberg, Germany. E-mail: peter.comba@aci.uni-heidelberg.de; Fax: +49-6226-546617*
[b]*Bundesanstalt für Materialforschung und-prüfung, Abteilung für Röntgenstrukturanalytik, Richard-Willstätter-Straße 11, D-12489 Berlin, Germany*
[c]*Helmholtz-Zentrum Dresden-Rossendorf, Institute of Radiopharmacy, D-01314 Dresden, Germany. E-mail: h.stephan@hzdr.de*
[d]*Technische Universität Dresden, Department of Chemistry and Food Chemistry, D-01062 Dresden, Germany*

†Electronic supplementary information (ESI) available: Details of the potentiometric titrations, solution *vs.* solid state electronic spectra, the CSD codes for structural comparison and details of the crystallographic analyses are given as ESI. CCDC 904928 and 904929. For ESI and crystallographic data in CIF or other electronic format see DOI: 10.1039/c2dt32356g

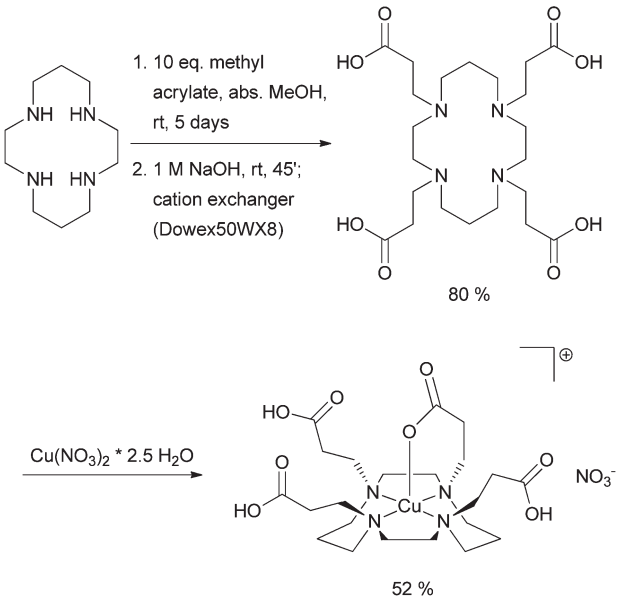

Chart 1 Structure and synthesis of H_4TETP and its Cu^{II} complex.

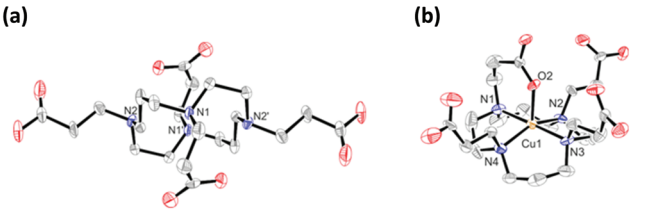

Fig. 1 Crystal structure of the free ligand H_4TETP (a) and $[Cu(H_3TETP)]^+$ (b). Thermal ellipsoids are shown at the 30% probability level. Protons, H_2O and counter ions are omitted for clarity.

Table 1 Selected structural parameters of $[Cu^{II}(H_3TETP)]^+$

Distance	Å	Angle	(°)
Cu–N1	2.058(6)	N1–Cu–N3	178.4(3)
Cu–N2	2.058(5)	N2–Cu–N4	151.2(2)
Cu–N3	2.112(6)	N1–Cu–O2	90.7(2)
Cu–N4	2.092(6)	N2–Cu–O2	103.6(2)
Cu–O2	2.110(5)	N4–Cu–O2	105.3(2)

Results and discussion

Synthesis and structure of the ligand and its copper(II) complex

H_4TETP was obtained in 80% yield by Michael addition of methyl acrylate to cyclam, followed by base hydrolysis of the resulting tetra ester.[23,26,27] Dropwise addition of an aqueous solution of $Cu(NO_3)_2 \cdot 2.5H_2O$ to a hot solution of H_4TETP in methanol–water yielded the copper(II) complex in 52% yield (see Chart 1).

Coordinated tetraazamacrocyclic ligands can adopt five *trans*-configurations (*trans*-I to *trans*-V), as well as two possible *cis*-configurations;[28] with cyclam, the most stable Cu^{II} complex has *trans*-III geometry (*R*,*R*,*S*,*S*-configurations of the coordinated secondary amine donors), with chair conformations of the six-membered and δ,λ conformations of the five-membered chelate rings. With substituted tertiary amine donors, other geometries have been observed; with Ni^{II} the tetramethylated cyclam complex has been shown to assume *trans*-I geometry (*R*,*S*,*R*,*S*-configuration of the amine donors), and this was interpreted on the basis of force field calculations to be a result of steric interactions between the methyl substituents.[29] The copper(II) coordination chemistry with the 6,13-bispyridyl substituted cyclam derivative is a rare case, where four different isomers could be isolated and structurally characterized (five- and six-coordinate Cu^{II} with different axial donor groups, *i.e.* two different forms of *trans*-I, *trans*-III, and a rare case of *trans*-IV with twist-boat conformations of the six-membered rings).[30] Typically, Cu^{II} complexes of tetraazamacrocyclic ligands in a *trans*-I configuration are five-, those in *trans*-III are six-coordinate (4 + 1 *vs.* 4 + 2 coordination geometry), and the former generally have shorter bonds to the axial donors than the latter.[30–32]

Interestingly, there are two structural isomers known of the copper(II) complex of the analogous cyclam-1,4,8,11-tetraacetic acid (H_4TETA):[13] both have two deprotonated and coordinated acetate groups, while the two others are protonated and dangling, and therefore the usual *trans*-III configuration and 4 + 2 coordination geometry is observed. However, in one of the isomeric structures, the Cu–N bonds are relatively short (2.06, 2.16 Å) with two relatively long axial bonds to the carboxylate oxygen atoms (2.27 Å). In the other isomer there are two distinct sets of Cu–N bonds (2.00, 2.38 Å) and relatively short bonds to the carboxylate oxygen atoms (2.02 Å), *i.e.* these structures may be understood as "Jahn–Teller isomers".[33,34] This indicates that the carboxylate donors of substituted cyclam-based ligands such as H_4TETA and H_4TETP (and the corresponding mono-, bis- and tris-substituted macrocycles) are relatively strong and may lead to unusual coordination geometries. It therefore came with no surprise that the complex crystallized is $[Cu(H_3TETP)]^+$, *i.e.* pentacoordinate, with three protonated and only one coordinated propionate, and has a *trans*-I configuration with the expected chair conformations of the six-membered and envelope conformations of the five-membered chelate rings. The structure of the molecular cation together with that of the metal-free ligand (see ESI† for details of these structures) is shown in Fig. 1 and relevant distances and angles of the complex are given in Table 1.

The four Cu–N bonds are relatively long for cyclam-type Cu^{II}–N distances but not unusual (see those of the H_2TETA-based complex discussed above; those of the *trans*-I structure of the bis-pyridine-substituted cyclam also mentioned above are 2.00 Å on average),[13,30] *i.e.* the in-plane ligand field is relatively weak. In addition, there is a significant angular distortion (see valence angles involving the metal center in Table 1); in fact, the structure is nearly half-way between square pyramidal and trigonal bipyramidal, $\tau = 0.45$ ($\beta = 178.4°$, $\alpha = 151.2°$),[35] and this is not unexpected for *trans*-I geometry with one coordinated propionate. The distance to the pseudo-axial carboxylate is relatively short for an axial Cu^{II}–O(carboxylate) bond

but again not unusual (see the cited distances in the case of the [Cu(H_2TETA)] complex above), *i.e.* there is a relatively weak in-plane and a relatively strong axial ligand field, leading to partial quenching of the pseudo-Jahn–Teller distortion. Therefore, based on the structural data one cannot expect a large stability of this complex, and this clearly has an influence on the biological properties (see the section on biodistribution below). A preliminary computational analysis suggests that the observed structure is enforced by the ligand and therefore is expected to be retained in solution[36–39] (see the section on spectroscopy below).

The observed structure of $[Cu(H_3TETP)]^+$ was compared to 30 structures of Cu^{II} complexes of cyclam derivatives in a *trans*-I configuration and with axial oxygen donors (see ESI† for a table with the relevant CCSD reference codes and the corresponding Cu^{II}–N/O distances). The average Cu–N distance of these structures is 2.05 Å which is similar to the average Cu–N distance of 2.08 Å for $[Cu(H_3TETP)]^+$. In 16 of these structures the axial O-donor is part of the cyclam platform with an (enforced) average Cu–O distance of 2.206 Å, 14 structures show a free axial O-donor with an average Cu–O distance of 2.324 Å. The relatively short Cu–O distance in $[Cu(H_3TETP)]^+$ therefore seems to be the most significant structural feature. Cu^{II}–cyclam complexes with a *trans*-I geometry and a pendant acetate donor have Cu–O distances of 2.252 Å (CSD-Reference Code: DESQUEX[40]) and 2.223 Å (CSD-Reference Code: TOKTAO[41]); a complex with a propionic acid ethylester axial donor has a Cu–O distance of 2.223 Å, (CSD-Reference Code: SALKUL[42]) and a Cu^{II} complex with four propyl alcohol substituents shows a Cu–O distance of 2.252 Å (CSD-Reference Code: RAQCIW[43]).

Solution chemistry

The stability of $[Cu(H_3TETP)]^+$ was studied by potentiometric titrations (see the Experimental Section and ESI†). With the high stability of these macrocyclic ligand complexes, as usual these experiments needed to involve competition titrations, and these were done with EDTA (EDTA = ethylenediaminetetraacetate).[44] Unfortunately, the results of these titrations did not allow us to accurately determine the complex stability (see ESI†). However, the log *K* value unambiguously is smaller than 18 and therefore, as expected (see above), significantly smaller than those of the corresponding Cu^{II} complexes of cyclam (log *K* = 28.1)[9] and H_4TETA (log *K* = 21.9).[44]

A thorough analysis of the ligand field spectra allows us to determine bonding parameters of transition metal complexes: with the angular overlap model (AOM) the ligand field can be analyzed in terms of e_σ and e_π values for all individual donors.[31,45] For copper(II) (d^9), coordinated in a distorted square-pyramidal geometry, four transitions are expected. A Gaussian analysis of the experimental solid state spectrum (see Fig. 2) reveals three transitions assigned to excitations from the degenerate d_{xz} and d_{yz} orbitals to the singly occupied $d_{x^2-y^2}$ orbital (611 nm), as well from the d_{xy} orbital (761 nm) and from the d_{z^2} orbital (1021 nm; see Table 2). The calculated transition energies obtained from AOM calculations, using the

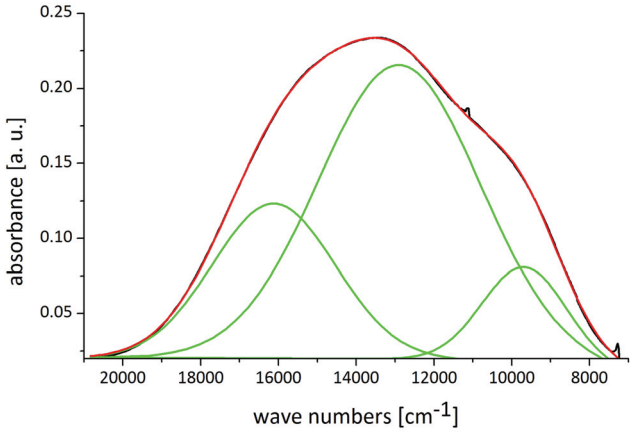

Fig. 2 Diffuse reflectance solid state UV-vis-NIR spectrum of crystalline [Cu^{II}(H_3-TETP)]NO_3 in alox (black curve) and Gaussian deconvolution of the experimental spectrum (green and red curves).

Table 2 Experimentally observed and computed transition energies of [Cu^{II}(H_3-TETP)](NO_3)

	Experimental		AOM	
Transitions	[cm^{-1}]	[nm]	[cm^{-1}]	[nm]
$d_{z^2} \rightarrow d_{x^2-y^2}$	9794	1021	10 370	964
$d_{x,y} \rightarrow d_{x^2y^2}$	13 140	761	14 134	708
$d_{xz,yz} \rightarrow d_{x^2-y^2}$	16 359	611	16 658; 17 359	600; 576

observed coordinates of the Cu^{II} center and the five donor groups and transferable AOM parameters, are in good agreement with the experimental values (Table 2; $e_\sigma \approx ad$(Cu–N);[6] ds orbital mixing: e_{ds} = 1/4 e_σ of the in-plane ligand field; for the Stevens-orbital factor *k* a value of 0.80 was assumed which results in a spin–orbit coupling constant for the complexed Cu^{II} ion of ζ = 662 cm^{-1}, free Cu^{II} ion: ζ = 828 cm^{-1}).[31,46,47] Importantly, the solution UV-vis-NIR spectrum, although not well resolved (see ESI†), is in qualitative agreement with the data given in Fig. 2 and Table 2. Moreover, the frozen solution EPR spectrum and the corresponding AOM-computed spin Hamiltonian parameters (see Fig. 3 for the experimental and simulated spectra and Table 3 for the parameters) also are in acceptable agreement. It emerges that the structure of the complex in solution is similar to that observed in the solid (see Fig. 1), with an in-plane ligand field (and Cu^{II}–N bonding) weakened by ligand-enforced distortions (relative to the basic cyclam platform), and with a relatively short Cu^{II}–carboxylate bond which is partially quenching the pseudo-Jahn–Teller distortion.

Radiolabeling and biodistribution

A tetra-branched peptide derivative of H_4TETP was shown to form a $^{64}Cu^{II}$ complex with a high enough *in vivo* stability to allow accumulation in HT-29 tumor xenotransplants.[27] However, complex formation kinetics of this peptide bioconjugate with Cu^{II} was relatively slow. In contrast, complex formation with the unsubstituted H_4TETP is fast in aqueous

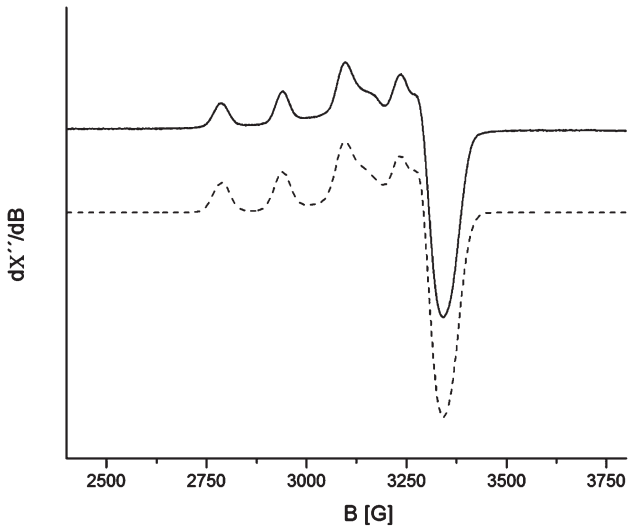

Fig. 3 Experimental X-band EPR spectrum of a 2 mM solution of $[Cu^{II}(H_3TETP)]$-NO_3 in methanol at 110 K (solid) and a simulated spectrum using XSophe (dashed).

Table 3 Experimentally observed and computed *g*- and *A*-tensors of $[Cu^{II}(H_3TETP)](NO_3)$

Experimental		AOM
$g_x = 2.0400$	$A_x = 25.00$	$g_x = 2.0492$
$g_y = 2.0911$	$A_y = 42.00$	$g_y = 2.0799$
$g_z = 2.2355$	$A_z = 156.00$	$g_z = 2.2372$

solution: upon addition of 1 equiv. of $Cu(NO_3)_2$ to H_4TETP (2 mM in water) the greenish complex $[Cu(H_3TETP)]^+$ was observed within few seconds. In order to achieve complete complex formation for radiolabeling experiments (low ligand concentration) a slightly increased temperature and reaction time were necessary. With 50 μg H_4TETP in 200 μL aqueous buffer solution the radiochemical yield (RCY) was >95% after 60 minutes at 37 °C (5 minutes: RCY ~ 80%).

In order to test the *in vivo* behavior of the ^{64}Cu-labeled H_4TETP in comparison to the analogously labeled acetate ligand H_4TETA, biodistributions were studied in rats (see Fig. 4). The data clearly demonstrate that the $[^{64}Cu(H_2TETA)]$ complex is excreted faster from the organism than the $[^{64}Cu(H_3TETP)]^+$ complex. $[^{64}Cu(H_2TETA)]$ is nearly exclusively eliminated *via* the renal route, while significant amounts of $[^{64}Cu(H_3TETP)]^+$ are accumulated in the liver, resulting in a substantial fraction eliminated *via* the hepatobiliary route. The activity uptake at 24 h after injection was lower in all organs for $[^{64}Cu(H_2TETA)]$ than for $[^{64}Cu(H_3TETP)]^+$. At 24 h after injection of $[^{64}Cu(H_2TETP)]^+$ most organs still show a substantial activity uptake but predominantly this happens in the kidneys and the liver. We assume that *in vivo* transchelation, due to the lower stability (see discussion of the structural data and solution coordination chemistry), and possible differences in the overall charge are reasons for the observed biodistribution pattern.

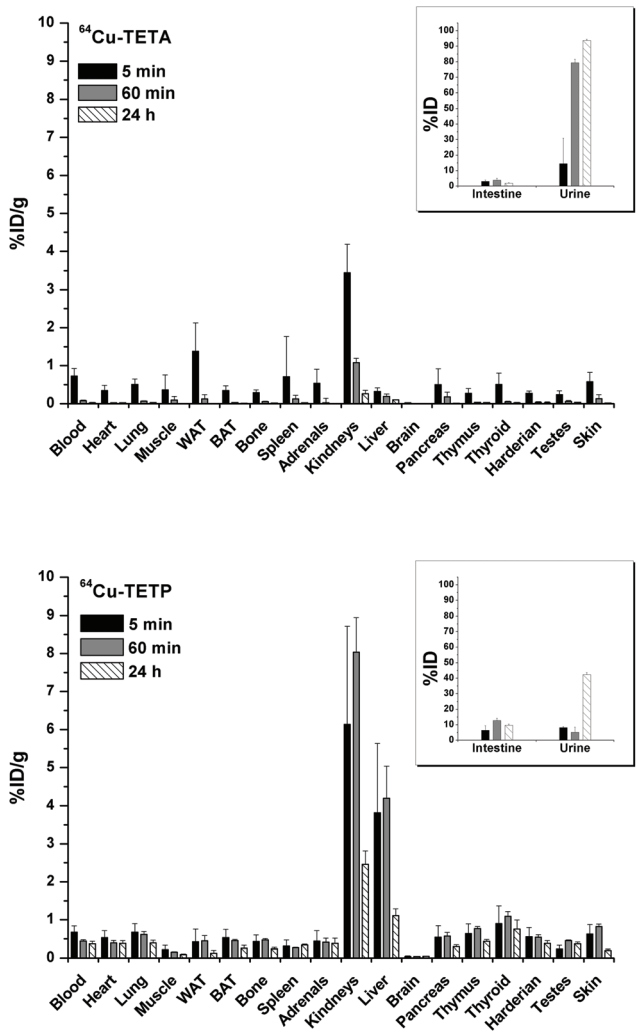

Fig. 4 Biodistribution data of ^{64}Cu-labeled H_4TETA (top) and H_4TETP (bottom) at 5 min, 60 min, and 24 h after injection (eight Kyoto–Wistar rats per time point, mean ± standard deviation).

Conclusion

$[Cu(H_3TETP)]^+$ has relatively long in-plane Cu–N bonds and a rather short bond to the axial carboxylate, leading to a coordination geometry which is nearly half-way between square-pyramidal and trigonal-bipyramidal; electronic and EPR spectroscopy, supported by ligand-field calculation, indicate that this structure is largely conserved in solution. While this is not entirely unusual or unexpected, and partially is due to the *trans*-I configuration, enforced by the four N-based substituents and by the six-membered chelate involving the coordinated propionate group, it is the ligand-enforced relatively weak in-plane and relatively strong axial bonding which lead to partial quenching of the pseudo-Jahn–Teller effect and a concomitant weakening of the bonding, and therefore to a relatively low complex stability. Potentiometric titrations support these assumptions, and the biodistribution data also point to a lower *in vivo* stability of the $[^{64}Cu(H_3TETP)]^+$ in

comparison to the [^{64}Cu(H$_2$TETA)] complex and therefore support the structural analysis.

Experimental section

Materials and methods

^{1}H- and ^{13}C-NMR were recorded on a 400 MHz Varian Inova spectrometer. The chemical shifts (δ, ppm) are relative to TMS or the solvent.

X-band EPR spectra (*ca.* 9 GHz) were recorded with a Bruker Biospin ELEXSYS E500 spectrometer. For measurements at 110 K in methanol, a Eurotherm temperature controller in conjunction with a liquid nitrogen flow through a system was used. Spin Hamiltonian parameters were determined from computer simulation of the experimental spectra using the XSophe-Sophe-XeprView computer simulation suite.[48,49]

UV-vis-NIR-spectra were recorded on a Jasco V-570 UV-vis-near-IR spectrophotometer. For the diffuse reflectance solid state spectrum the isolated complex was triturated with alox (Al_2O_3).

The production of ^{64}Cu was performed at a PET cyclotron, similar to those described for the ^{64}Cu–^{61}Co-production process.[50–52] For the ^{64}Ni(p,n)^{64}Cu nuclear reaction, 15 MeV protons of a Cyclone® 18/9 with a beam current of 12 μA for 150 min were used. The complete separation of ^{64}Cu and ^{61}Co was confirmed by gamma-ray spectroscopy. Nickel targets were prepared by electrodeposition of enriched ^{64}Ni (99.6%) on gold disks at amounts of 95–120 mg. The plated diameter was 7 mm, matching more than 80% intensity of the cyclotron proton beam, as measured by autoradiography of a ^{nat}Ni disk irradiated with 15 MeV protons to induce the ^{nat}Ni(p,x)^{57}Ni reaction. The yields of the nuclear reaction ^{64}Ni(p,n)^{64}Cu constituted between 3.6–5.2 GBq (EOB) with specific activities of 150–250 GBq μmol^{-1} Cu.

Elemental analyses were recorded on a EURO EA CHNS-Elemental Analyzer (HEKAtech GmbH). Electrospray ionization mass spectrometry (ESI-MS) was carried out using a Micromass Tandem Quadrupole Mass spectrometer (Quattro LC).

The single crystal X-ray data collection was carried out on a Bruker AXS SMART diffractometer at room temperature using MoKα radiation (λ = 0.71073 Å), monochromatized by a graphite crystal. The data reduction was performed by using the Bruker AXS SAINT and SADABS packages.[53] The structure was solved by direct methods and refined by full-matrix least squares calculation using SHELX97.[54] Anisotropic thermal parameters were employed for non-hydrogen atoms. The hydrogen atoms were treated isotropically with U_{iso} = 1.2 times the U_{eq} value of the parent atom. Crystal data and refinement details are summarized in the ESI.† CCDC-904928 and CCDC-904929 contain the supplementary crystallographic data for this paper.

Radio-TLC chromatograms were scanned using a Radioisotope Thin Layer Analyzer (Rita Star, raytest). Radio-HPLC characterization was performed by using a Knauer System consisting of a pump Wellchrom HPLC K100, UV-detector K-2501, software Chromgate 2.8, activity detector Raytest Ramona Star, ZIC®-HILIC column (di2chrom Marl, Germany), 150 × 4.6 mm, 200 Å, 3.5 μm, eluent: A: acetonitrile, B: 0.1 M ammonium acetate (pH = 6.8), 5 min 20% B, 5 minutes from 20% B to 90% B, 20 minutes 90% B, 0.5 mL min^{-1}.

Syntheses

Cyclam, *TETA*·4HCl·4H$_2$O and Cu(NO$_3$)$_2$·2.5H$_2$O were purchased from Sigma Aldrich. H$_4$TETP was synthesized following a previously reported procedure.[27] Analytical data were in agreement with those described in the literature.

[*Cu*(*H$_3$TETP*)](*NO$_3$*): To a hot solution of TETP·0.5H$_2$O (77.4 mg, 0.16 mmol) in methanol–water (1 : 1, 1.5 mL) was added dropwise 1.5 mL of an aqueous solution of Cu(NO$_3$)$_2$·2.5H$_2$O (35 mg, 0.16 mmol). The solution was stirred at room temperature for 2.5 h. After complete evaporation of all solvents, the residue was taken up in a mixture of ethanol–water (35 : 1, 3.6 mL) and subjected to crystallize to diethyl ether diffusion. The resulting blue crystals were collected, washed twice with diethyl ether and dried (50 mg, 52% yield). ESI-MS (*m*/*z*): Calculated for $C_{22}H_{39}CuN_4O_8$ 552.1[M + H]$^+$. Found: 552.45[M + H]$^+$, 276.9[M + 2H]$^{2+}$; Anal Calcd for $C_{22}H_{39}N_4O_8CuNO_3 \times 1.5H_2O$: C 41.28, H 10.94, N 6.61, found: C 41.34, H 10.83, N 6.55. Visible electronic spectrum: λ_{max} (H$_2$O)/722 nm (ε = 210 M^{-1} cm^{-1}).

Radiolabeling of H$_4$TETA and H$_4$TETP with ^{64}Cu

Labeling of H$_4$TETA and H$_4$TETP (50 μg ligand dissolved in 0.01 M MES-NaOH buffer, pH = 5.5) was carried out by addition of 20 MBq [^{64}Cu]CuCl$_2$ 200 μL followed by 60 min incubation at 37 °C. Formation of the radiocopper complexes was verified by Radio-TLC using a mobile phase methanol: 2 M ammonium acetate (1 : 1) on a RP-18 silica plate (^{64}CuCl$_2$, R_f = 0; ^{64}Cu-TETA, R_f = 0.9; [^{64}Cu(H$_3$TETP)]$^+$, R_f = 0.35). Radio-HPLC analyses were done to determine the purity and labeling yield of the radioactive compound (^{64}CuCl$_2$, t_R = 5.5 min, [^{64}Cu(H$_2$TETA)], t_R = 16.1 min, [^{64}Cu(H$_3$TETP)]$^+$, t_R = 17.1 min).

Biodistribution

All animal experiments were carried out in male Wistar rats (Kyoto-Wistar strain; aged 7–8 weeks, 130–170 g; Harlan Winkelmann GmbH, Borchen, Germany) according to the guidelines of the German Regulations for Animal Welfare. The protocol was approved by the local Ethical Committee for Animal Experiments. Animals were kept under a 12 h light-dark cycle and fed with commercial animal diet and water *ad libitum*.

For biodistribution studies, the animals were injected into the tail vein under anaesthesia (inhalation of 9% (v/v) desflurane (Suprane, Baxter, Germany) in 40% oxygen/air (gas flow 0.5 L min^{-1})). The injection volume of either [^{64}Cu(H$_3$TETP)]$^+$ or [^{64}Cu(H$_2$TETA)] (1 MBq; radiochemical purity >95%; specific activity: 10 MBq μg^{-1}) dissolved in electrolyte solution E-153 (Serumwerk Bernburg, Germany), pH 7.2, was 0.5 mL. The biodistribution was determined in groups of eight rats sacrificed by heart puncture under ether anaesthesia at 5 min, 60 min, and 24 hours post injection (*p.i.*). Organs and tissues of

interest were rapidly excised, weighed, and the radioactivity was determined in a Wallac WIZARD Automatic Gamma Counter (PerkinElmer, Germany) and a dose calibrator (Dose Calibrator ISOMED 2000, MED Nuklear-Medizintechnik Dresden GmbH, Germany), respectively. The activity of ^{64}Cu in the tissue samples was decay-corrected and calibrated by comparing the counts in tissue with the counts in aliquots of the injected radiotracer that had been measured both in the gamma counter and the dose calibrator and at the same time. The accumulated radioactivity in organs and tissues was calculated as either the percentage of the injected dose per gram tissue (%ID g^{-1} tissue) or, for both intestine and urine, the percentage of the injected dose (%ID).

Acknowledgements

Financial support by the initiative and networking fund of the Helmholtz Association on the Virtual Institute "Functional nanomaterials for multimodality cancer imaging" (Nano-Tracking, Agreement Number VH-VI-421) is gratefully acknowledged.

References

1 R. Weissleder, *Science*, 2006, **312**, 1168.
2 S. M. Rice, C. A. Roney, P. Daumar and J. S. Lewis, *Semin. Nucl. Med.*, 2011, **41**, 265.
3 V. Ambrosini, M. Fani, S. Fanti, F. Forrer and H. R. Maecke, *J. Nucl. Med.*, 2011, **52**(Suppl.), 42S.
4 M. Shokeen and C. J. Anderson, *Acc. Chem. Res.*, 2009, **42**, 832.
5 T. J. Wadas, E. H. Wong, G. R. Weisman and C. J. Anderson, *Chem. Rev.*, 2010, **110**, 2858.
6 M. T. Ma and P. S. Donnelly, *Curr. Med. Chem.*, 2011, **11**, 500.
7 M. S. Cooper, M. T. Ma, K. Sunassee, K. P. Shaw, J. Williams, R. L. Paul, P. S. Donnelly and P. J. Blower, *Bioconjugate Chem.*, 2012, **23**, 1029.
8 M. D. Bartholomä, *Inorg. Chim. Acta*, 2012, **389**, 36.
9 R. J. Motekaitis, B. E. Rogers, D. E. Reichert, A. E. Martell and M. J. Welch, *Inorg. Chem.*, 1996, **35**, 3821.
10 I. M. Helps, D. Parker, J. Chapman and G. Ferguson, *J. Chem. Soc.*, 1988, 1094.
11 J. Chapman, G. Ferguson, J. F. Gallagher, M. C. Jennings and D. Parker, *J. Chem. Soc., Dalton Trans.*, 1992, 345.
12 K. S. Woodin, K. J. Heroux, C. A. Boswell, E. H. Wong, G. R. Weisman, W. Niu, S. A. Tomellini, C. J. Anderson, L. N. Zakharov and A. L. Rheingold, *Eur. J. Inorg. Chem.*, 2005, 4829.
13 J. D. Silversides, C. C. Allan and S. J. Archibald, *Dalton Trans.*, 2007, 971.
14 D. N. Pandya, J. Y. Kim, J. C. Park, H. Lee, P. B. Phapale, W. Kwak, T. H. Choi, G. J. Cheon, Y.-R. Yoon and J. Yoo, *Chem. Commun.*, 2010, **46**, 3517.
15 L. M. Lima, D. Esteban-Gomez, R. Delgado, C. Platas-Iglesias and R. Tripier, *Inorg. Chem.*, 2012, **51**, 6916.
16 P. Comba, L. M. Engelhardt, J. M. Harrowfield, E. Horn, A. M. Sargeson, M. R. Snow and A. H. White, *Inorg. Chem.*, 1985, **24**, 2325.
17 P. V. Bernhardt, L. M. Bramley, L. M. Engelhardt, J. M. Harrowfield, D. C. R. Hockless, B. R. Korybutdaszkiewicz, E. R. Krausz, T. Morgan, A. M. Sargeson, B. W. Skelton and A. H. White, *Inorg. Chem.*, 1995, **34**, 3589.
18 A. M. Sargeson, *Coord. Chem. Rev.*, 1996, **151**, 89.
19 N. Di Bartolo, A. M. Sargeson and S. V. Smith, *Org. Biomol. Chem.*, 2006, **4**, 3350.
20 G. Gasser, L. Tjioe, B. Graham, M. J. Belousoff, S. Juran, M. Walther, J. U. Kunster, R. Bergmann, H. Stephan and L. Spiccia, *Bioconjugate Chem.*, 2008, **19**, 719.
21 S. Juran, M. Walther, H. Stephan, R. Bergmann, J. Steinbach, W. Kraus, F. Emmerling and P. Comba, *Bioconjugate Chem.*, 2009, **20**, 347.
22 S. Fähnemann, H. Stephan, J. Steinbach, C. Haaf and P. Comba, *Nucl. Med. Biol.*, 2010, **37**, 678.
23 V. Bulach, D. Mandon, J. Fischer and R. Weiss, *Inorg. Chim. Acta*, 1993, **210**, 7.
24 C. Lecomte, V. Dahaoui-Gindrey, H. Chollet, C. Gros, A. K. Mishra, F. Barbette, P. Pullumbi and R. Guilard, *Inorg. Chem.*, 1997, **36**, 3827.
25 M. Meyer, V. Dahaoui-Gindrey, C. Lecomte and R. Guilard, *Coord. Chem. Rev.*, 1998, **178–180**, 1313.
26 H. Stephan, G. Geipel, D. Appelhans, G. Bernhard, D. Tabuani, H. Komber and B. Voit, *Tetrahedron Lett.*, 2005, **46**, 3209.
27 A. Röhrich, R. Bergmann, A. Kretzschmann, S. Noll, J. Steinbach, J. Pietzsch and H. Stephan, *J. Inorg. Biochem.*, 2011, **105**, 821.
28 B. Bosnich, C. K. Poon and M. L. Tobe, *Inorg. Chem.*, 1965, **4**, 1102.
29 T. W. Hambley, *J. Chem. Soc., Dalton Trans.*, 1986, 565.
30 P. Comba, S. M. Luther, O. Maas, H. Pritzkow and A. Vielfort, *Inorg. Chem.*, 2001, **40**, 2335.
31 P. Comba, T. W. Hambley, M. A. Hitchman and H. Stratemeier, *Inorg. Chem.*, 1995, **34**, 3903.
32 P. Comba, P. Jurisic, Y. D. Lampeka, A. Peters, A. I. Prikhod`ko and H. Pritzkow, *Inorg. Chim. Acta*, 2001, **324**, 99.
33 P. Comba, A. Hauser, M. Kerscher and H. Pritzkow, *Angew. Chem., Int. Ed.*, 2003, **42**, 4536, (*Angew. Chem.*, 2003, **115**, 4675).
34 P. Comba, S. Pandian, H. Wadepohl and S. Wiesner, *Inorg. Chim. Acta*, 2011, 422 (*Wolfgang Kaim 60 birthday special*).
35 A. W. Addison, T. N. Rao, J. Reedijk, J. van Rijn and G. Verschoor, *J. Chem. Soc., Dalton Trans.*, 1984, 1349.
36 J. E. Bol, C. Buning, P. Comba, J. Reedijk and M. Ströhle, *J. Comput. Chem.*, 1998, **19**, 512.
37 A. Bentz, P. Comba, R. J. Deeth, M. Kerscher, H. Pritzkow, B. Seibold and H. Wadepohl, *Inorg. Chem.*, 2008, **47**, 9518.

38 M. Atanasov, P. Comba, B. Martin, V. Müller, G. Rajaraman, H. Rohwer and S. Wunderlich, *J. Comput. Chem.*, 2006, **27**, 1263.
39 Our current force fields[36,37] are not well tuned for axial carboxylates and therefore, this result is only qualitative. DFT calculations are not expected to lead to accurate enough predictions,[38] see the section on spectroscopy.
40 H. Aneetha, Y.-H. Lai, S.-C. Lin, K. Pannerselvam, T.-H. Lu and C.-S. Chung, *J. Chem. Soc., Dalton Trans.*, 1999, 2885.
41 L. Yu-Juan, Y. Xiao-Ming, H. Bing and S. Li-Jun, *J. Chem. Soc., Dalton Trans.*, 1996, 2885.
42 D. Tschudin, A. Riesen and T. A. Kaden, *Helv. Chim. Acta*, 1989, **72**, 131.
43 A. Channa and J. W. Steed, *Dalton Trans.*, 2005, 2455.
44 E. T. Clarke and A. E. Martell, *Inorg. Chim. Acta*, 1991, **190**, 27.
45 B. N. Figgis and M. A. Hitchman, *Ligand Field Theory and its Applications*, Wiley-VCH, Weinheim, New York, 2000, p. 354.
46 P. Comba, *Coord. Chem. Rev.*, 1999, **182**, 343.
47 P. Comba, *Coord. Chem. Rev.*, 2000, **200–202**, 217.
48 D. Wang and G. R. Hanson, *J. Magn. Reson., Ser. A*, 1995, **117**, 1.
49 D. Wang and G. R. Hanson, *Appl. Magn. Reson.*, 1996, **11**, 401.
50 F. Szelecsényi, G. Blessing and S. M. Qaim, *Appl. Radiat. Isot.*, 1993, **44**, 575.
51 D. W. McCarthy, R. E. Shefer, R. E. Klinkowstein, L. A. Bass, W. H. Margeneau, C. S. Cutler, C. J. Anderson and M. J. Welch, *Nucl. Med. Biol.*, 1997, **24**, 35.
52 M. A. Avila-Rodriguez, J. A. Nye and R. J. Nickles, *Appl. Radiat. Isot.*, 2007, **65**, 1115.
53 G. M. Sheldrick, Universität Göttingen, 2002.
54 G. M. Sheldrick, *Acta Crystallogr., Sect. A: Fundam. Crystallogr.*, 2008, **64**, 112.

